Extraction of Blood Vessels Geometric Shape Features with Catheter Localization and Geodesic Distance Transform for Right Coronary Artery Detection.

Ahmed Hawas

Extraction of Blood Vessels Geometric Shape Features with Catheter Localization and Geodesic Distance Transform for Right Coronary Artery Detection

Ahmed R. Hawas[1], Mohamed Elsayed Elsetiha[2], Heba A. El-Khobby[3], Amira S. Ashour[3]

[1]Electronics and Electrical Communication Engineering Department, Faculty of Engineering, Tanta University, 31527, Egypt - email: ahm.hawas@gmail.com
[2]Department of Cardiology, Faculty of Medicine, Tanta University, 31527, Egypt
[3]Electronics and Electrical Communication Engineering Department, Faculty of Engineering, Tanta University, 31527, Egypt

Abstract: **X-ray angiography is considered the standard imaging sensory system for diagnosing coronary artery diseases. For automated, accurate diagnosis of such diseases, coronary vessels' detection from the captured low quality and noisy angiography images is challenging. It is essential to detect the main branch of the coronary artery, to resolve such limitations along with the problems due to the sudden changes in the lumen diameter, and the abrupt changes in local artery direction. Accordingly, this paper solved these limitations by proposing a computer-aided detection system for the right coronary artery (RCA) extraction, where geometric shape features with catheter localization and geodesic distance transform in the angiography images through two parts. In part 1, the captured image was initially preprocessed for contrast enhancement using singular value decomposition-based contrast adjustment, followed by generating the vesselness map using Jerman filter, and for further segmentation the K-means was introduced. Afterward, in part 2, the geometric shape features of the RCA, as well as the skeleton gradient transform, and the start/end points were determined to extract the main blood vessel of the RCA. The analysis of the skeletonize image was performed using Geodesic distance transform to examine all branches starting from the predetermined start point and cover the branching till the predefined end points. A ranking matrix, and the inverse of skeletonization were finally carried out to get the actual main branch. The performance of the proposed system was then evaluated using different evaluation metrics on the angiography images. The results validated the dominance of the suggested system for extracting the main vessel achieving Dice values improvements within the range 2% - 30% compared to using the traditional methods.**

Keywords: **Angiography, right coronary artery, vessel segmentation, geometric shape features extraction, skeleton gradient transform, Geodesic distance transform**

I. INTRODUCTION

In cardiovascular analysis, fast and accurate allocation of the arterial main branch is considered an essential prerequisite for further diagnostic procedures, including feature-based classification or registration as well as for the three-dimensional reconstruction of the coronary artery (CA). Automated computer-aided diagnosis system in cardiovascular analysis-based cardiovascular examinations has a valuable impact on the speed and precision of diagnosing CA diseases. Segmentation, detection, and visualization of the vessels in the coronary artery angiography (CAA) images assist the physicians to diagnose cerebrovascular/cardiovascular

diseases. In practice, treatment requires diagnosis which in turn needs analysis and judgement on the CAA images by extracting initially the central-line and the main branch of CA [1].

For detecting the main branch, direct investigative center/main-line detection or pixel-based segmentation can be applied to yield an independent representation of the background and the foreground. Several vessel's feature extraction techniques, including pixel classification techniques, hysteresis thresholding, and eigenvalues of Hessian matrix (HM) have been implemented [2, 3]. However, in the existence of non-uniform illumination, such techniques provide disparate pixels' clusters rather than single connected arterial branch for further tracing the main branch by direct extraction of the features of interest using sequential search through exploring the pixels located close to the vasculature of the arterial segments. Typically, CA vascular extraction can be performed using edge-/region-based segmentation procedures.

Various studies have been conducted for center-line extraction of the CA based on dynamic search, nevertheless, such techniques take long time, which does not meet the clinical real-time requirements. Other limitations include the complex structure of the CA, and the uneven gray-scale distribution of CAA images that complicate the center-line extraction of the CA vessels [4]. Generally, the centerline of the CA vessel looks like a ridge-line collecting series of ridge points representing the local extrema points of the pixels' brightness in an image at a certain direction. In the CAA images, such centerline exists like gray extreme values of the perpendicular vessel's direction. To detect such ridge points, the image's gradient and the HM can be calculated [5]. Also, HM has been used to evaluate the blood vessels' characteristics with a multiscale vessel enhancement filtering for CA extraction [6]. In addition, tracing the ridge-points in the multi-scale space of the CAA images has been conducted for extracting the center-line of the CA by identifying the primary seed points by applying the gradient vector flow field with fast marching schemes [7]. Besides, there are some techniques introduce a new post processing stage for HM's response for better and accurate results while identifying the vessel tree like connectivity filter [8]. However, other techniques depend on fine tuning parameters for vesselness filter [9, 10].

II. RELATED WORK

The preceding reported techniques in the Introduction section concluded that no methods can be conducted to compute accurately the distal regions of the CA centerlines owing to the calcification and narrowing of the blood vessels in the CA. The performance of such detection methods varies in consistent with their parameters' values. Furthermore, several existing schemes ignore the effect of the vessels' shape, which provides significant information for medical diagnosis.

Several studies have been caried out for vessels segmentation in angiograms. For example, Dehkordi et al. [11] implemented a local feature fitting energy with active contour (AC) in [11] based on the HM enriched with information about pixel energy level while choosing the domain subset for AC processing to extract the whole vessel tree. The findings indicated the robustness of this model to various initial contours, however, it suffers from the limitations of the AC.

In contrast, low contrast X-ray angiogram images have been segmented by combining HM with flux flow measuring to identify vessel pixels as designed in [12] with accuracy of 96% for major vessels segmentation. Other study by Hernandez-Vela et al. [13] has been realized using the main shape features for CA to identify the vesselness tree. It identified the main seed points which have the maximum vesselness response and start to search for the paths between the seed points to format the vessel tree. However, this method suffers from the high computational time requirements.

To overwhelm these shortcomings, the proposed system develops a fast and accurate center-line extraction based on the catheter localization with vessel geometric shape features extraction for right coronary artery (RCA) detection. This paper targets solving the problem of main branch extraction by proposing a novel automatic tracking system-based vessel extraction method that detects the RCA using vessel geometric shape features. In this proposed system, a searching method is applied to calculate geometric shape features for each vessel starting from predefined point. In addition, a skeleton method is used with the segmented image to determine the existing branches based on their characteristics for final determination of the main artery branch.

The organization of the coming sections includes the procedure of the proposed system, followed by the experimental results with discussion. Then, finally, the conclusion of the conducted work is summarized in the conclusion section.

III. METHODOLOGY

In this paper, a new automated tracking system was proposed for detecting the RCA blood vessel based on vessel geometric shape features. In the proposed system, each vessel's profile was determined followed by a searching algorithm to find the fitted branch that has the matched geometric shape features with the blood vessel features. Initially, a starting point was defined by searching for the catheter location on the original CAA image, which automatically leads to the vessel start point. The skeletonized image version was also computed from the segmented image which is analyzed to examine all branches starting from pre-

determined start point till all available ends and branching points. During the branching scan process, branch characteristics are being determined, including branch length, diameter, and distance from a reference point. Finally, a decision making was evaluated using the ranking of these characteristics leading to the main artery branch of interested.

In the proposed system, before extracting the main RCA, which is the main objective of this paper, other stages were applied as in [10], namely (Part 1): i) preprocessing using singular value decomposition- based contrast adjustment (SVD), ii) generating the vesselness map using Jerman filter [14], and iii) segmentation using K-means to extract artery vessels from the enhanced low contrast CAA images (refer to [10, 14] for the mathematical details on theses sequential stages). These stages were then followed by the main stages of the proposed system to extract the main RCA branch using the geometric shape features, which are (Part 2): a) skeletonization, b) start points determination, c) geometric shape features extraction, and d) main branch selection. Figure 1 illustrates the general stages of the overall proposed system.

Figure 1 demonstrates that the overall proposed system includes two parts. In Part 1, a preprocessing stage to separate the vessels and the background was applied as the angiography images have low contrast value using contrast adjustment using SVD, and equalization using contrast-limited adaptive histogram equalization (CLAHE), followed by smoothing using guided filter that preserve the sharp boundaries, and histogram stretching. Afterward, the vesselness map was generated based on multiscale analysis by convolving the original image with a Gaussian filter, then the HM was measured at each point [10]. The HM provides information of the direction of vessels to ensure the continuity of main pixels on the blood vessels and their neighbors. Jerman [14] filter is based on HM that offered a robust vesselness to bifurcations. After generating the vesselness map, the K-means was conducted for segmentation. The segmented image contains all segmented vessels, while the X-ray angiography examination is only interested on the stenosis at main arteries with ignoring all other branches, so the proposed stages in "Part 2" are introduced to select main artery from all segmented vessels as described in detail as follows.

A. *Main artery extraction*

1) *Geometric Shape Features*

By visual inspection of the RCA images in the used dataset and compare the characteristics of the main artery "RCA" to surrounding vessels, it is found that the RCA has two main characteristics, namely the longest length, and the largest diameter (width).
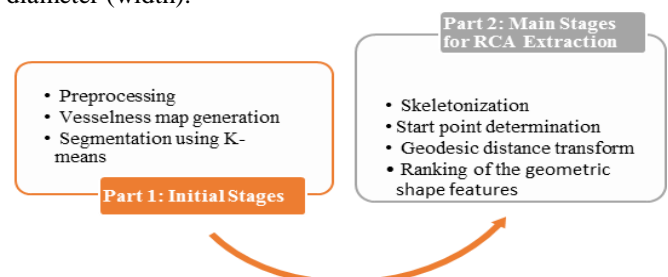

Figure 1. Stages of the overall proposed system.

Moreover, its end point is the closest point to the lower-right corner as well-known clinically, where the stent is attached only to main arteries. Thus, any used segmentation method of the angiography images must have capabilities to extract the main vessel and ignore other vessels. The proposed system provides a generic way to extract main artery from any image based on its main features using the following stages.

2) Skeletonization

Since it is inexpedient to deal with the segmented image directly for detecting and objects having specific characteristics, conversion must be taken place to facilitate a searching stage based on these specific geometric shape features in terms of the computational and complexity prospective. As the geometric shape features of the RCA includes its longest length, and largest diameter (width) compared to its surrounding vessels, the skeletonization is applied in the proposed system. Generally, the skeletonization is used for limiting the foreground regions to a skeletal trace which mainly conserves the extent/connectivity of the original region with discarding most of the original foreground pixels. The most reliable skeletonization technique, the most consistent and precise results can provide.

In the proposed system, a skeleton gradient transform (SGT) was applied before using the standard skeletonization for better skeletonization results. The SGT provides a transient image based on the intensity of each pixel/point on the vessel that is proportional to the degree of evidence being a point on the skeleton. The first step to calculate SGT image is to define the junction points in the image. Each point of the image is examined using weighted matrix P and calculate the neighborhood joint W which is given by:

$$W_{(x,y)} = \begin{pmatrix} i_{(x-1,y-1)} & i_{(x-1,y)} \\ i_{(x,y-1)} & i_{(x,y)} \end{pmatrix} .* P \qquad (1)$$

where $P = \begin{pmatrix} 1 & 8 \\ 2 & 4 \end{pmatrix}$ as the values of the weighted matrix P is chosen to describe the number and position of neighbors for a specific pixel point $i_{(x,y)}$, i.e., if the $W_{(x,y)}$ equal to 15, this means pixel value $i_{(x,y)}$ is 1 and has three neighbors and if the $W_{(x,y)}$ equal to 10, this means pixel value $i_{(x,y)}$ is zero and has two neighbors. Any pixel $i_{(x,y)}$ has $W_{(x,y)}$ not equal to zero (has no neighbor and its value is zero) or 15 (by considering three neighbors and its value is 1) is considered as a junction point $J_{(x,y)}$. Junction points are scanned based on clockwise direction and label each junction point with its rank across edge $JR_{(x,y)}$ where the first junction point will have rank equal 1 then second one will have rank equal 2 and so on till scan all junction points. Total count of junction points presents the perimeter of the edge $EdgLen$, which is expressed as follows:

$$EdgLen = lengt\square(J_i) \qquad (2)$$

The second stage before generating the SGT version is to find the minimum distance d_{min} for each true pixel point $(I_{(x,y)} = 1)$ and any junction points for 4 directions, namely North-EAST "NE", North-West "NW", South-East "SE", and

South-West "SW". Therefore, the minimum distance can be formulated as follows:

$$d_{min} = \min(\forall_{jnx,jny} dist_{Dir}((x,y),(jx`,jy`))) \qquad (3)$$

where the distance at the different directions can be calculated as follows:

$$dist_{Dir} = (x - jx`)^2 + (y - jy`)^2$$
$$forDir = NE \rightarrow jx` = jx and jy` = jy$$
$$forDir = NW \rightarrow jx` = jx and jy` = jy + 1 \qquad (4)$$
$$forDir = SE \rightarrow jx` = jx + 1 and jy` = jy$$
$$forDir = SW \rightarrow jx` = jx + 1 and jy` = jy + 1$$

The rank for each junction points that presenting the minimum distance at a specific direction $JR_{(x,y)}(NE, NW, SE, SW)$ is calculated. From these ranks, the largest perimeter span $LPS_{(x,y)}$ can be easily premeditated by ordering these ranks and subtract the first and last one. For each true pixel point, the final SGT can be determined by subtracting the edge perimeter $EdgLen$ from its largest perimeter span using the following formula:

$$SGT(x,y) = EdgLen - LPS(x,y) \qquad (5)$$

The final stage to generate the accurate skeleton version is to apply a standard skeletonization method [15] on the generated SGT version. From the skeleton version, it is very easy to determine the branching and end point for future searching steps.

3) Vessel start-point determination

To facilities the searching process of the main RCA with reducing the computational time, the proposed system applied a strategy to determine one of the start or end point of the detected vessel that matches the geometric shape features. Since the catheter is always sited at the upper-center section of the angiography image, it is used to represent the starting point of the main artery as it is responsible for the pushing agent while recording the images. Accordingly, determining the location of the catheter can figure out the location of the starting point of the main RCA. The proposed system uses the cross-correlation [16] between the segmented image and a template image that shows a sample version of catheter. The template image of the catheter can be easily constructed by cropping it from any ground truth image. The location of the catheter can be located by looking for the region having the highest correlation value compared to the template, where the correlation coefficient is calculated using the following expression [16]:

$$CC(u,v) = \frac{\sum_{x,y}[im(x,y) - \bar{im}_{u,v}][TM(x-u,y-v) - \bar{TM}]}{\left\{ \sum_{x,y}[im(x,y) - \bar{im}_{u,v}]^2 \sum_{x,y}[TM(x-u,y-v) - \bar{TM}]^2 \right\}^{0.5}} \qquad (6)$$

where, im and TM are the original and template images, respectively, $\bar{TM}$ is the mean of the template and $\bar{im}_{u,v}$ is the mean of $im_{(x,y)}$ in the region under the template.

To provide the accurate position of the catheter at the upper part of the image, the normalized two-dimensional cross-

correlation that was calculated [16], is leading to the region that has the starting point of the main artery. Then, the Euclidean distance is calculated for each branching and end points. The closest point is considered the starting point.

4) Geodesic distance transform and inverse skeletonization

From the above stages, the skeletonized image version is computed from the segmented image and determined the starting point of the main branch. The final stage is to determine the end point based on the main branch geometric features (the longest, and largest branch). Then, an evaluation analysis is taken placed to evaluate all branches starting from predetermined start point to all end and branching points to conclude the main branch as follows.

To enhance the performance and accuracy of the search procedure, a reference matrix "REF" is created having the same size of the image and filled by zeros except the interested end point set to 1. Then, the geodesic distance transform [17] is computed from the segmented image (SI), and the seed positions specified by "REF", where the regions in SI having true values signify valid regions which could be traversed in the calculation of the distance transform. However, the regions in SI having false values characterize the constrained regions which could not be traversed. Every pixel has true value in SI, the geodesic distance transform [17] assigns a number referring to the constrained distance amongst that pixel and the nearest true pixel in "REF". Accordingly, the output matrix D containing geodesic distances can be represented as follows [17]:

$$D = \begin{cases} |x_1 - x_2| + (\sqrt{2} - 1)|y_1 - y_2|, & |x_1 - x_2| > |y_1 - y_2| \\ (\sqrt{2} - 1)|x_1 - x_2| + |y_1 - y_2|, & ot\square erwise. \end{cases} \quad (7)$$

where D is the distance between (x_1, y_1) and (x_2, y_2).

Then, the maximum distance of D represents the longest path in the SI, so an automatic tracking is starting from start point towards the end point under the condition that the next point must have geodesic distance less than the current one till it reaches another endpoint. At this stage, the proposed system knows two important information regarding the CAA image, namely i) the number of branches, and ii) the exact skeleton points for each branch. Based on the number of points representing the branch's skeleton, the proposed system can detect the longest branch which is one of RCA geometric shape features.

To guarantee that the previous detected branch using the length as a geometric shape feature is the final main RCA, other remaining decision making based on the second geometric feature (i.e., the average diameter of a vessel) is required. Hence, to determine the vessel diameter at any point of the skeleton, initially the orientation of the object is determined under specific mask size [5*5], where the point of interest is located at the middle. By knowing the orientation of a specific point, the norm direction of this point is determined. Subsequently, a counter is proposed to count each pixel point that has value equal to 1 starting for the interested point till reach the boundary point on the segmented image on the norm direction as well as for the opposite direction, which will signify the diameter vessel at this point. During scanning the

detected branches, the geometric shape features characteristics are determined (i.e., branch length, diameter, and distance from a reference point local near the lower right corner). The final selection of the main branch is based on a proposed ranking equation for these features.

All branches are being sorted ascendingly based on each geometric shape features (i.e. length, diameter and distance from a reference point). For example, the shortest branch will assign to rank number 1, while the longest one will have the highest rank based on the number of branches are being evaluated. The same is followed in terms of the diameter, and distance from a reference point. The decision making DM is then evaluated using the ranking of the geometric shape features of the branch to finally conclude the main artery branch (i.e. RCA), which physician is interested based on the value of DM as follows:

$$DM = max(\forall(\frac{LenR_n * DiaR_n}{DisR_n})) \quad (8)$$

where $LenR_n$ is the length rank, $DiaR_n$ is the diameter rank, and $DisR_n$ is the reference distance rank. The branch with the maximum DM is being selected as the main branch that represents the main artery branch.

B. Performance evaluation metrics of proposed system

Numerous quantitative metrics are calculated to evaluate the performance of the proposed vesselness segmentation methodology, namely Jaccard index (JAC), Dice coefficient, sensitivity, specificity, and accuracy, which are defined as follows [18]. The JAC is a statistical metric that compares the diversity between sample sets as follows:

$$JAC(O,T) = \frac{A_O \cap A_T}{A_O \cup A_T} \quad (9)$$

where $\cap$ and $\cup$ are the intersection and union of two sets, correspondingly, in addition, A_o and A_T are the segmented, and the ground-truth images enclosed by the boundaries O and T; respectively. The value of 1 specifies complete similarity, while JAC value of 0 specifies no similarity. In addition, the Dice index (F1-score) is measured to compare the similarity of any two sets, which is given as follows for two sets O and T:

$$DIC(O,T) = \frac{2|A_O \cap A_T|}{|A_O| + |A_T|} \quad (10)$$

Likewise, the sensitivity, specificity, and accuracy are associated to the recognition of the main branch. The sensitivity designates the true positive rate viewing the success of the proposed system to predict the main branch, which is stated as follows:

$$Sensitivity = \frac{|TP|}{|TP| + |FN|} \quad (11)$$

where TP is true positives and FN is false negatives. The specificity designates the true negative rate viewing the ability of the proposed system to predict the other regions as follows:

$$Specificity = \frac{|TN|}{|TN| + |FP|} \quad (12)$$

where TN is true negatives and FP is false positives. The accuracy is the true results proportion either positive or negative that measures the reliability degree of a diagnostic test using the following formula:

$$Accuracy = \frac{|TP| + |TN|}{|TP| + |TN| + |FP| + |FN|} \quad (13)$$

IV. RESULTS AND DISCUSSION

C. Dataset Acquisition

X-ray angiography images were acquired during cardiology catheter examination on 200 patients in OM EL-Kore Cardiac Center, Tanta, ElGharbia, Egypt, which is described in detail in [10]. The ground-truth images were labeled by an expert, where, in this work, we detected the main branch of the RCA view. Figure 2 shows samples of the original images of the RCA X-ray angiogram images in the RCA view, and the corresponding ground-truth images, in the upper, and lower row, respectively.
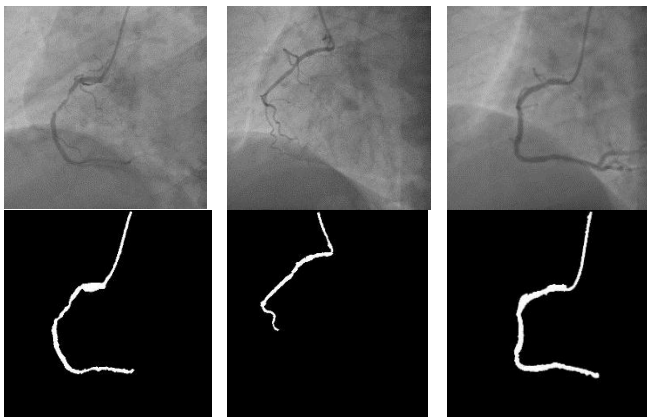

Figure 2. Samples of the original images, and their ground-truth images, in the upper, and lower row, respectively.

D. Results of proposed system: Part 1

As previously explained in the Methodology section, the proposed system in Part 1 has 3 main stages/modules. The results of each stage in Part 1 are demonstrated and discussed as follows.

1) Results of preprocessing stage

Firstly, the original image passed through the preprocessing stage. Figure 3 illustrates the more brightness added to the image especially at the left upper corner after contrast adjust without effect any other information related to the image.

Figure 3 illustrates that the contrast of the image is enhanced using the SVD. Then, this enhanced image is passed through a histogram equalizer by applying the CLAHE method with its default parameters' setting for the tile size of 8x8. In addition, the trial-and-error approach was followed to determine the clip limit value of 0.0047. Figure 4 shows the visual display of the resultant image after the histogram equalization process.

Figure 4 demonstrates the contrast improvement with clear visibility of the arteries structure. The final preprocessing stage

is to perform smoothing, and histogram stretching on the image illustrated in Fig. 5.

Figure 5 proves that the image contrast is properly enhanced, and the main artery is completely visible after finalizing the whole preprocessing steps.
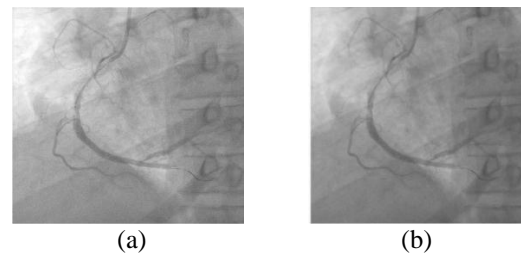

Figure 3. Result of contract adjustment using SVD, where (a) the original image, and (b) the image after SVD processing.
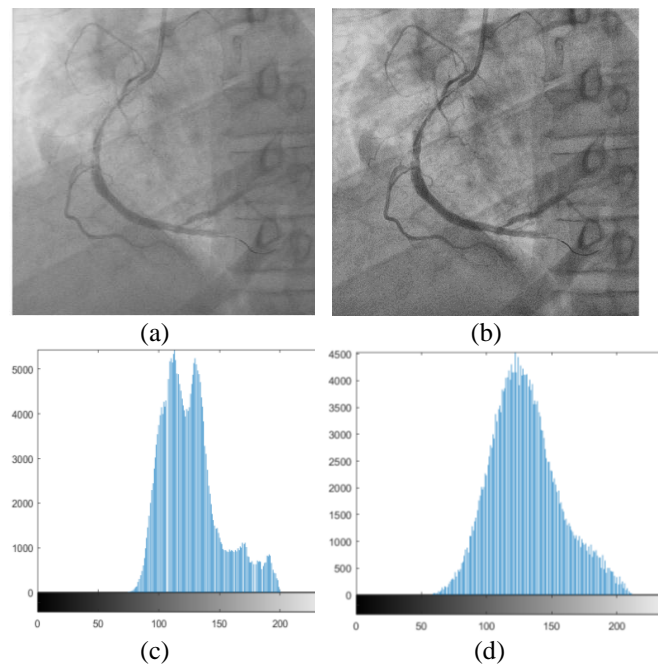

Figure 4. Result of histogram equalizer using CLAHE, where (a) input image, (b) enhanced contrast image, (c) histogram of the input image, and (d) histogram of enhanced image.
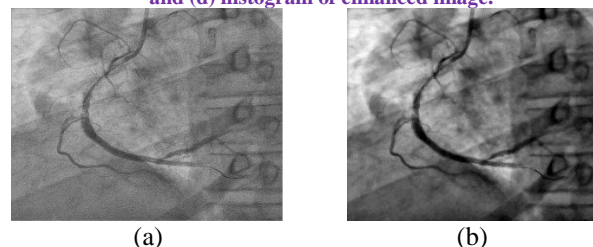

Figure 5. Result of preprocessing, where (a) output image of CLAHE, and (b) the final image after smoothing and histogram stretching.

2) Results of vesselness map generation and segmentation stages

The next stage is only concerned with segmentation of the main artery. Figure 6(a) shows the vesselness map response when using Jerman filter. The results show high sensitivity for any change on the spatial domain, where it can be considered

a strength point if it is combined with selective technique with high efficiency. Figure 6(b) shows the result after applying K-means with initial cluster points [50 180] which represent displacement by 20% from zero value (near value for background) and from half gray scale value 127.5 (near value for foreground) respectively.

Finally, a searching analysis is performed to extract the largest connected component to be used for the next stage as shown in Fig. 7. Figure 7 demonstrates that the segmented regions include too many small vessels that are not interested based on physician advice. So, in the next stage the proposed technique tries to eliminate these unwanted branches plus extract only main vessel by applying part 2 of the proposed system.
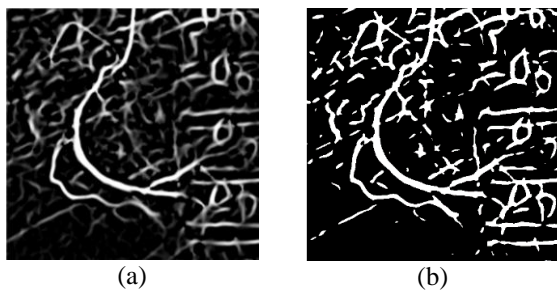

Figure 6. Result of Jerman filer, where (a) vesselness map response, and (b) segmented object after using K-means.

Figure 7. Segmentation results

E.   Results of proposed system: Part 2

Generally, the main artery is noticeable by the naked eye; nevertheless, stenosis detection is a complicated and essential process for detecting and determining the oblique percentage for further diagnosis and treatment. It is required to determine the main branch and the diameter of the stenosis to choose the correct stent dimension for the patient automatically. Detecting and recognizing the main branch simplify and guide the stenosis calculations. In the present study, the angiography images are employed to detect the main RCA branch for precise computerized identification and clinical decision support.

3) Results of Geodesic distance transform and skeletonization stage

In part 2, the target is to extract the main vessel by performing deep analysis on the skeleton image. Before applying the standard skeletonization, there is an important mapping called SGT to be used instead of the segmented image for better skeletonization results. Figure 8 illustrates the

difference between applying the standard skeletonization on the segmented image directly and applying the same technique on the SGT version of the image.

Figure 8 (b) shows a very smooth version by removing very small branches that will cause unnecessary processing while searching for the main vessel compared to Fig. 8(a). Based on the skeleton image, it is easy to determine the end, and the branching points. The next stage is to determine the starting point based on the correlation between the upper part of the segmented image, and a predefined image for the stent as show in Fig. 9. Figure 9 depicts that the region with high correlation value enclosed the area containing the starting point of the main vessel.
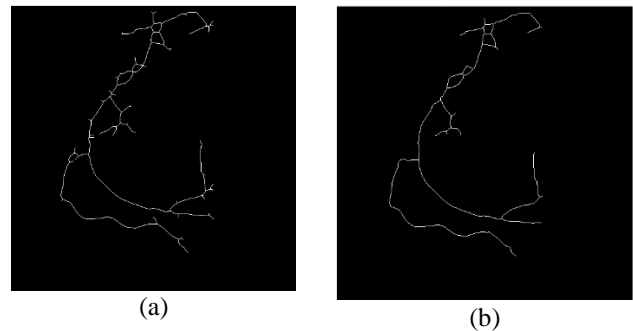

Figure 8. Results of applying standard skeletonization on: (a) the segmented image directly, and (b) the SGT image.
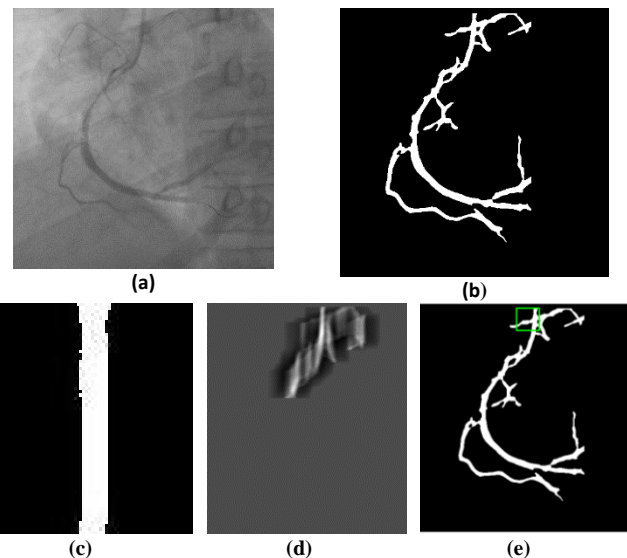

Figure 9. Start point selection, where (a) Original image, (b) segmented image, (c) predefined stent image, (d) correlation result response, and (e) the area of high correlation value bounded in green box.

4) Results of geometric shape features extraction and inverse skeletonization stages

After determining the starting point, an extensive search analysis is conducted to find the main branch's end point that matches the geometric shape features (i.e., longest length, largest diameter, and the nearest one to the lower center points). Once the ranking process is completed, the main branch is finally determined and the inverse skeletonization is being

performed to extract the main vessel as shown on Fig. 10 as standard stage call "skeleton gradient transform" (SGT) for accurate results.

Figure 10 displays that this stage provides a transient image version based on the intensity at each point that is proportional to the degree of evidence that this should be a point on the skeleton. Figure 10 validates the recognition results using the proposed technique in comparison to the ground-truth images. In the Fig. 11(d), the detected boundaries are marked in blue, and the ground-truth results are in red.

Figure 11 establishes that the detection results are accurately matched with the corresponding ground-truth. The proposed system is accurately detected the main branch regions even with different shapes and sizes.

(a)   (b)

Figure 10. Finding the main artery RCA, where (a) the detected path after performing ranking process and (b) segmented image after applying inverse skeleton process.

F. *Performance evaluation results*

Different assessment measurements were calculated for evaluating the execution of the proposed system and its ability for detecting the main RCA branch as reported in Table 1. Table 1 accounts the average values and the standard deviation (SD) of the assessment metrics of the proposed system after preprocessing using Jerman for skeletonization, and K-means for final extraction of the main branch of RCA. The comparative study in Table 1 compares the proposed system performance for detection with and without conducting the stage of main branch extraction over the dataset.

Table 1 indicates that the proposed system provides a significant enhancement compared to the traditional methods. An improvement in the JAC average value by 25% was measured with accurate capability of the proposed system to detect the main RCA vessel. Also, the DSC and JAC values are less than SEN, SPEC and ACC values, where the interested object is very small compared with its background leading to high values for SEN, SPEC and ACC even if the system is inaccurate.

Other comparative study using different combinations of the used vesselness and segmentation techniques in part 1 of the proposed system were conducted. Thus, the proposed system for extracting the main RCA vessel is also combined with other vesselness technique, such as Frangi with using the regional growing for segmentation to evaluate the system reliability across different techniques as reported in Table 2.

Table 2 shows a major enhancement added for each method to detect only the main artery. The only exception is when using the Frangi with the regional growing as there is minor enhancement as the parameters used is optimized to generate

only main artery only that is why there is no significant enhancement (the same results are presented in Fig. 12).
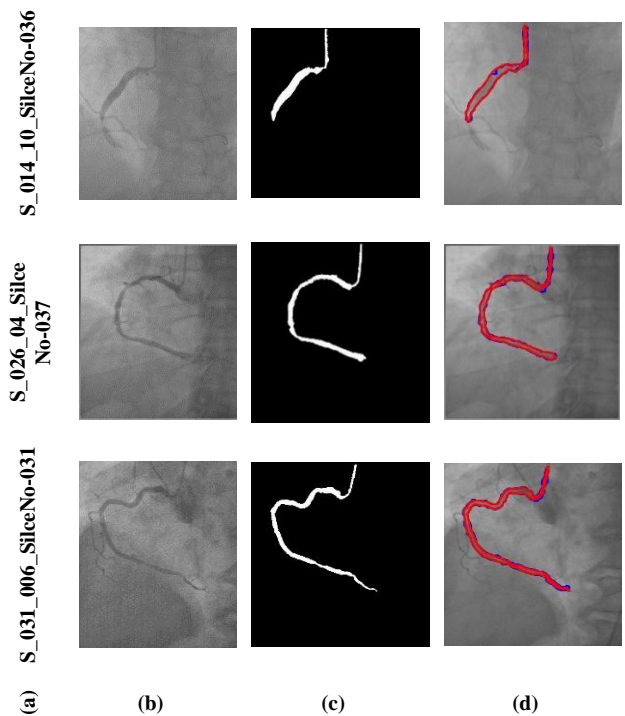

(a)   (b)   (c)   (d)

Figure 11. Final RCA main branch selection results, where (a) the original image ID number, (b) the original image, (c) the ground-truth image, and (d) the detected main branch using the proposed system.

Table 1. The performance of segmentation using the proposed system with reference to ground-truth boundaries (average ± SD).

Proposed system	JAC	DSC	SEN	SPEC	ACC
Part1 only	49.87 ±14.72	65.03±1 5.74	87.68±1 7.04	97.89± 1.32	97.61± 1.49
Part1 and part2	75.26±5. 29	85.78±3. 44	87.99±7. 81	99.63± 0.2	99.33± 0.14

In Table 2, and Fig. 12, J stands for Jerman vesselness filter, F stands for Frangi vesselness filter, K stands for K-means segmentation, R stands for the regional growing segmentation, P1 stands for apply part1 only, P1P2 stands for apply part1 then P2 in the proposed system.

Table 2. Comparison of using part 2 for extracting the main branch with different vesselness and segmentation techniques in part 1 of the proposed system.

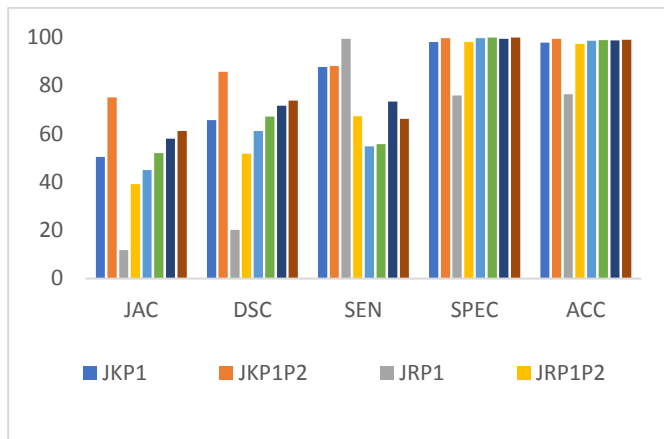| Main RCA extraction system	JAC	DSC	SEN	SPEC	ACC
JKP1	50.46	65.58	87.65	98	97.72
JKP1P2	75	85.61	88.01	99.62	99.33
JRP1	11.78	20.2	99.27	75.82	76.36
JRP1P2	39.08	51.78	67.27	97.93	97.21
FKP1	44.96	61.14	54.78	99.59	98.58
FKP1P2	52	67.06	55.69	99.85	98.74
FRP1	57.9	71.6	73.3	99.3	98.6
FRP1P2	61.07	73.76	66.15	99.82	98.94

Figure 12 Comparison of using part 2 for extracting the main branch with different vesselness and segmentation techniques in part 1 of the proposed system.

Table 3. Numerical comparison of segmentation methods with the proposed system

Ref.	Used method	Dice Score	Accuracy	Sensitivity	Specificity
Hernandez-Vela, C. Gatta, et al.[13]	Centerline with Graph Cut	69.75	97.20	63.51	99.03
Taghizadeh Dehkordi, A.M. Doost Hoseini, et al.[11]	HM + Active contours	68.50	96.91	67.88	98.41
Felfelian, H.R. Fazlali, et al.[12]	HM with Flux flow	72.79	97.09	74.92	98.32
Nasr-Esfahani, S. Samavi, et al.[19]	CNN	75.62	97.27	79.35	98.91
Nasr-Esfahani, N. Karimi, et al.[20]	CNN	81.51	97.93	86.76	98.59
Proposed system	**Geometric shape features**	**85.78**	**99.33**	**87.99**	**99.63**

*The best results are in bold.

G. Comparative study with state-of-the-art

The proposed system is also evaluated against others state-of-the-art (SOTA) for vessel extraction in X-ray angiograms [11-13]. In [11], active contour was applied on HM filter response, also in [12], the authors also applied hessian filter combined with flux flow results, while in [13] the graph cut and centerline for segmentation were applied. The proposed system is also evaluated in comparison with other SOTA that used deep learning networks, where for example [19] applied deep learning by using one conventional neural network (CNN), while [20, 21] used two CNNs. the first stage for CNN is used to construct the vessel probability map based on local and global features then this probability map is combined with edge detection map to second CNN stage for vesselness detection.

Table 3 indicates that the suggested system surpasses the other methods in terms of the segmentation metrics. It is notable that the exact recognition of the vessel parts by the proposed system leads to high Dice of 85.78%, which exceeds the 2nd best technique by variance about 4%. The sensitivity, and accuracy of the proposed system are 87.99%, and 99.33%, respectively, which outpaced the current SOTA by accomplishing almost 4% higher Dice.

V. CONCLUSION

Computer-assisted detection/segmentation of coronary arteries is exciting challenging process due to the low contrast and class mismatch of artifacts in X-ray angiographic images. Various studies have been conducted to solve these limitations. This study introduced a novel main artery detection system based on geometric shape features of the main artery in the X-ray angiographies. In the proposed system, each vessel's geometric features were determined then the perfect match vessel based on ranking equation is considered as the main artery. To speed up the searching computation, First, a starting point was defined by locating the catheter position on the segmented image. This will automatically lead to the starting point of the vessel.

A skeletonized image version is also computed from the segmented image and analyzed to explore all branches starting from a given starting point to all available endpoints and branch points. During the scanning process, each vessel branch determines its properties such as junction length, diameter, and distance from the predefined point. Finally, decision-making was assessed using a ranking of features that led to major arterial branches of interest. The outcomes of the suggested system demonstrated its robustness to deal with any vesselness filter. The proposed system provides higher evaluation metrics than the traditional ways. These features manage the vesselness selection based on artery length, diameter and its position that achieved the highest JAC in the segmentation procedure. Five measurements were calculated for comparing the performing of the proposed method with other procedures. The findings demonstrated the dominance of the proposed system with an average 85.78% dice across the outcomes of other techniques with distinct sizes, shapes, and homogeneity of the main artery.

Conflicts of Interest: The authors declare that there is no conflict of interest.

REFERENCES

[1] Li, Z., Zhang, Y., Liu, G., Shao, H., Li, W., and Tang, X., *A robust coronary artery identification and centerline extraction method in angiographies.* Biomedical Signal Processing and Control, 2015. **16**: p. 1-8.

[2] Aach, T., *Vessel Segmentation in Angiograms using Hysteresis Thresholding.* Conference on Machine VIsion Applications, 2005: p. 8-11.

[3] Rodrigues, L.C., and M. Marengoni, *Segmentation of optic disc and blood vessels in retinal images using wavelets, mathematical morphology and Hessian-based multi-scale filtering.* Biomedical signal processing and control, 2017. **36**: p. 39-49.

[4] Li, Z., Zhang, Y., Gong, H., Liu, G., Li, W., and Tang, X., *An automatic and efficient coronary arteries extraction method in CT angiographies.* Biomedical Signal Processing and Control, 2017. **36**: p. 221-233.

[5] Pudov, V., and Y.N. Dragoshanskii. *Formation of the magnetic domain structure and properties of magnetic cores under conditions of ordered laser deformations.* in *Doklady Physics.* 2017. Springer.

[6] Wang, S., B. Li, and S. Zhou. *A segmentation method of coronary angiograms based on multi-scale filtering and region-growing.* in *2012 International Conference on Biomedical Engineering and Biotechnology.* 2012. IEEE.

[7] Cui, H., and Y. Xia, *Automatic coronary centerline extraction using gradient vector flow field and fast marching method from CT images.* IEEE Access, 2018. **6**: p. 41816-41826.

[8] Rodrigues, E.O., Rodrigues, L. O., Machado, J. H., Casanova, D., Teixeira, M., Oliva, J. T., ... , and Liatsis, P., *Local-Sensitive Connectivity Filter (LS-CF): A Post-Processing Unsupervised Improvement of the Frangi, Hessian and Vesselness Filters for Multimodal Vessel Segmentation.* Journal of Imaging, 2022. **8**(10): p. 291.

[9] Mahapatra, S., Agrawal, S., Mishro, P. K., and Pachori, R. B., *A novel framework for retinal vessel segmentation using optimal improved frangi filter and adaptive weighted spatial FCM.* Computers in Biology and Medicine, 2022. **147**: p. 105770.

[10] 1Hawas, A.R., Elsetiha, M. E., El-Khobby, H., and Ashour, A., *Optimized Adaptive Frangi-based Coronary Artery Segmentation using Genetic Algorithm.* Journal of Engineering Research, 2022. **6**(5): p. 177-183.

[11] Taghizadeh Dehkordi, M., Doost Hoseini, A. M., Sadri, S., and Soltanianzadeh, H., *Local feature fitting active contour for segmenting vessels in angiograms.* IET Computer Vision, 2014. **8**(3): p. 161-170.

[12] 1Felfelian, B., Fazlali, H. R., Karimi, N., Soroushmehr, S. M. R., Samavi, S., Nallamothu, B., and Najarian, K., *Vessel segmentation in low contrast X-ray angiogram images.* in *2016 IEEE International Conference on Image Processing (ICIP)*. 2016. IEEE.

[13] Hernandez-Vela, A., Gatta, C., Escalera, S., Igual, L., Martin-Yuste, V., Sabate, M., and Radeva, P., *Accurate coronary centerline extraction, caliber estimation, and catheter detection in angiographies.* IEEE Transactions on Information Technology in Biomedicine, 2012. **16**(6): p. 1332-1340.

[14] Jerman, T., Pernuš, F., Likar, B., and Špiclin, Ž., *Enhancement of vascular structures in 3D and 2D angiographic images.* IEEE transactions on medical imaging, 2016. **35**(9): p. 2107-2118.

[15] Castleman, K.R., *Digital image processing*. 1996: Prentice Hall Press.

[16] Yoo, J.-C., and Han, T. H. , *Fast normalized cross-correlation.* Circuits, systems and signal processing, 2009. **28**(6).

[17] Toivanen, P.J., *New geodosic distance transforms for gray-scale images.* Pattern Recognition Letters, 1996. **17**(5): p. 437-450.

[18] Ashour, A.S., Hawas, A. R., Guo, Y., and Wahba, M. A., *A novel optimized neutrosophic k-means using genetic algorithm for skin lesion detection in dermoscopy images.* Signal, Image and Video Processing, 2018. **12**(7): p. 1311-1318.

[19] Nasr-Esfahani, E., Samavi, S., Karimi, N., Soroushmehr, S. R., Ward, K., Jafari, M. H., ... and Najarian, K., *Vessel extraction in X-ray angiograms using deep learning*. in *2016 38th Annual international conference of the IEEE engineering in medicine and biology society (EMBC)*. 2016. IEEE.

[20] Nasr-Esfahani, E., Karimi, N., Jafari, M. H., Soroushmehr, S. M. R., Samavi, S., Nallamothu, B. K., and Najarian, K., *Segmentation of vessels in angiograms using convolutional neural networks.* Biomedical Signal Processing and Control, 2018. **40**: p. 240-251.

[21] Nasr-Esfahani, E., Karimi, N., Jafari, M. H., Soroushmehr, S. M. R., Samavi, S., Nallamothu, B. K., and Najarian, K., *Segmentation of vessels in angiograms using convolutional neural networks.* Biomedical Signal Processing and Control, 2018. **40**: p. 240-251.